



ELSEVIER

Contents lists available at ScienceDirect

Journal of Membrane Science

journal homepage: www.elsevier.com/locate/memsci

Acetate based Supported Ionic Liquid Membranes (SILMs) for CO₂ separation: Influence of the temperature

E. Santos*, J. Albo, A. Irabien

Departamento de Ingeniería Química y Química Inorgánica, Universidad de Cantabria, Avda. de los Castros s/n., 39005 Santander, Spain



ARTICLE INFO

Article history:

Received 4 August 2013

Received in revised form

8 October 2013

Accepted 12 October 2013

Available online 21 October 2013

Keywords:

CO₂/N₂ separation

Room Temperature Ionic Liquids

Supported Ionic Liquid Membranes

Gas permeation

Solution–diffusion

ABSTRACT

Supported Ionic Liquid Membranes (SILMs) were prepared with the acetate based Room Temperature Ionic Liquids (RTILs) 1-ethyl-3-methylimidazolium acetate ([Emim][Ac]), 1-butyl-3-methylimidazolium acetate ([Bmim][Ac]) and the monomer vinylbenzyl trimethylammonium acetate ([Vbtma][Ac]) in order to perform the selective separation of carbon dioxide (CO₂) from nitrogen (N₂). The RTILs were supported in a polyvinylidene fluoride porous membrane and permeation experiments were performed in the temperature range 298–333 K. Gas permeability increases with temperature while an increase in temperature leads to a decrease in the CO₂/N₂ selectivity for all the studied RTILs. CO₂ solubility was evaluated in the range 298–333 K and atmospheric pressure using thermogravimetric techniques. Diffusion coefficients were calculated based on the solution–diffusion theory using gas permeability and solubility data. The temperature influence on the gas permeability, solubility and diffusivity are well described in terms of the Arrhenius–van't Hoff exponential relationships.

© 2013 Elsevier B.V. All rights reserved.

1. Introduction

The use of Supported Ionic Liquid Membranes (SILMs) for the selective separation of gases has received growing attention during recent years. In a SILM system, Room Temperature Ionic Liquids (RTILs) are immobilized inside the porous matrix of a polymeric or inorganic support. RTILs are organic salts liquid at room temperature showing a large variety of properties such as negligible vapor pressure, thermal stability at high temperatures or non-flammability [1], making them very attractive as immobilized phase in SILMs. The use of RTILs reduces the problem of solvent evaporation that may occur in conventional Supported Liquid Membranes (SLMs), allowing for obtaining liquid membranes with a higher stability [2]. Additionally, RTILs can be synthesized as task-specific solvents by the appropriate selection of the cation or anion in their structure [3] resulting in enhanced properties such as the gas solubility. The possibility of synthesize new RTILs with desired properties provides the opportunity for creating an ideal solvent for each potential application.

RTILs have received interest in CO₂ selective separations where the separation of CO₂ from mixtures containing N₂ is of great interest in power generation applications associated with the purification of flue gas streams. CO₂ permeability and CO₂/N₂ selectivity are the fundamental parameters characterizing the gas separation using membrane based technologies. There is a general trade-off between both parameters identified by the “upper

bound” limit observed for different polymeric materials in gas separation [4,5]. The development of new materials exceeding this line is a challenge in CO₂/N₂ separation.

There are several works available in the literature where SILMs were studied for CO₂/N₂ separation. Scovazzo et al. [6] report the gas permeability at 303 K of CO₂ and N₂ and the corresponding selectivities through a porous hydrophilic polyethersulfone (PES) support with different immobilized RTILs. They reported CO₂ permeabilities in the range of 350–920 barrers and CO₂/N₂ ideal selectivity ranged from 15 to 61. Bara et al. [7] obtained CO₂ permeabilities varying from 210 to 320 barrers and CO₂/N₂ separation factors between 16 and 26. Mixed-gas permeabilities and selectivities for CO₂/N₂ were also reported by Scovazzo et al. [8]. Cserjési et al. [9] investigated the use of SILMs prepared with 12 different types of RTILs immobilized in a hydrophilic polyvinylidene fluoride (PVDF) support. CO₂ permeabilities varied in the range of 94–750 barrers while CO₂/N₂ ideal selectivity ranged from 10.9 to 52.6. Neves et al. [10] studied the effect of the different cation alkyl chain length on the gas permeability. Gas permeability increases approximately by a factor of 2 with an increase in the cation alkyl chain length and the CO₂/N₂ ideal selectivity ranged from 22 to 39. Finally, Jindaratamee et al. [11] studied the permeability of CO₂ through imidazolium based ionic liquid membranes supported with a polyvinylidene fluoride (PVDF) porous membrane. They reported CO₂ permeabilities in 303–343 K temperature range varied from 120 to 445 barrers, with an ideal CO₂/N₂ selectivities from 42 to 86.

The selection of a suitable solvent is essential for the technical and economical viability of the CO₂ absorption where the solubility is the property of interest and the main selection criteria which

* Corresponding author: Tel.: +34 942 206749; fax: +34 942 201591.
E-mail address: santosse@unican.es (E. Santos).

has been the objective of many papers. The solubility of light gases such as CO₂ has been widely studied in RTILs. RTILs containing the acetate anion have been studied in the literature showing a strong absorption for CO₂. Maginn et al. [12] reported for the first time CO₂ solubility studies in the ionic liquid 1-butyl-3-methylimidazolium acetate ([Bmim][Ac]) showing very high CO₂ solubility. Chinn et al. [13] have proposed the CO₂/[Bmim][Ac]/water system for CO₂ capture. Shifflet et al. [14–18] have widely studied the phase behavior of CO₂ in 1-ethyl-3-methylimidazolium acetate [Emim][Ac] and 1-butyl-3-methylimidazolium acetate [Bmim][Ac] at temperatures ranging from 283 to 348 K and pressures up to 2 MPa. Bhargava et al. [19] and Steckel [20] performed ab initio calculations of the interaction between CO₂ and the acetate ion. Finally, Shi et al. [21] performed both simulation and experimental studies to separate mixtures of CO₂ and H₂ using [Emim][Ac] ionic liquid. Additionally, the use of polymeric ionic liquids (PILs) exhibits several times higher CO₂ absorption capacity than conventional monomeric Room Temperature Ionic Liquids (RTILs) due to faster CO₂ absorption and desorption rates [22]. The highest CO₂ solubility values and CO₂/N₂ selectivities can be achieved in the tetraalkylammonium poly(ionic liquid) p-[Vbtma] recently studied in the literature in combination with different anions [22,23].

In this work, the influence of the temperature on CO₂ and N₂ permeability and CO₂ solubility was investigated. SILMs including three acetate based RTILs were prepared in order to evaluate the CO₂/N₂ separation performance from 298 to 333 K. The CO₂ solubility was evaluated at 298–333 K and atmospheric pressure. The diffusion coefficients were calculated using gas permeability and solubility data applying the solution–diffusion hypothesis. The temperature dependence was described by using the Arrhenius or the van't Hoff equation in order to discuss the solubility and diffusivity contribution on the gas permeability through SILMs.

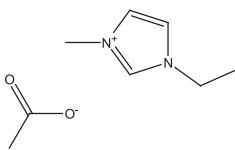
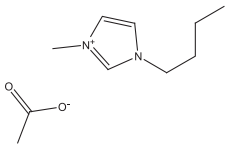
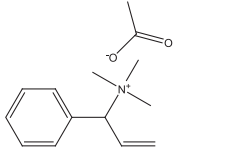
2. Experimental

2.1. Materials

The RTILs used in the present work were 1-ethyl-3-methylimidazolium acetate ([Emim][Ac]), 1-butyl-3-methylimidazolium acetate ([Bmim][Ac]) and (Vinylbenzyl)trimethylammonium acetate ([Vbtma][Ac]). [Emim][Ac] (assay \geq 96.5%, C₈H₁₄N₂O₂ CAS no. 143314-17-4) and [Bmim][Ac] (assay \geq 96%, C₁₀H₁₈N₂O₂ CAS no. 284049-75-8) they were supplied by Sigma Aldrich and used without further purification while [Vbtma][Ac] was synthesized in the *Faculdade de Farmácia, Universidade de Lisboa (Portugal)*. A solution of [Vbtma][Cl] (5 g, 0.0236 mol) in methanol (10 mL) was passed through a column with Amberlite IRA-400 (OH) resin. A solution of acetic acid (1 equiv., 0.1418 g, 0.0236 mol) in methanol was slowly added to [Vbtma][OH] obtained from the column and the mixture was stirred at room temperature for 30 min. The solvent was removed under vacuum. The RTIL was stirred under vacuum ($<$ 1 mmHg) at 60 °C overnight. (Vinylbenzyl)trimethylammonium acetate was obtained (5.4 g, 99.8%). Their molecular weight, density, viscosity and decomposition temperature are listed in Table 1. The density was determined using an automatic densimeter (Mettler Toledo DM40) at 298 K while viscosity data was obtained from the literature [24,25]. The density is in good agreement with the ones reported in the literature [24,25].

The thermal properties of the ionic liquids were determined by using thermogravimetric analysis (TGA). TGA analyses were carried out using a TGA-60H Shimadzu Thermobalance in a N₂ atmosphere at temperatures ranging from the room temperature to 873 K with a heating rate of 5 K min⁻¹. From the TGA curves shown in Fig. 1 it can be concluded that they are thermally stable up to 445 K under N₂ atmosphere which suggests that all of these RTILs have good thermal stabilities. A one-stage thermal decomposition process was observed

Table 1
Main characteristics of the studied RTILs.

Ionic liquid	Molecular structure	Molecular weight (g mol ⁻¹)	Density (g cm ⁻³ , 298 K)	Viscosity (cP, 298 K)	T _{onset} (K)
[Emim][Ac]		170.21	1.098	143.61 [24]	481.35
[Bmim][Ac]		198.26	1.052	24.82 [25]	496.93
[Vbtma][Ac]		235.32	1.015	–	445.1

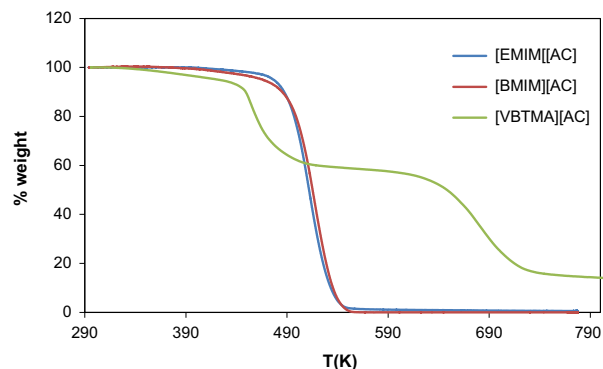


Fig. 1. TGA analyses for the for [Emim][Ac], [Bmim][Ac] and [Vbtma][Ac].

for [Emim][Ac] and [Bmim][Ac] while a two-stage decomposition was observed for the monomer [Vbtma][Ac]. The onset temperature (T_{onset}) calculated as the intersection of the baseline weight from the beginning of the experiment and the tangent of the weight vs. temperature curve as decomposition occurs was determined for each RTIL and is reported in Table 1.

The polymeric membrane selected as support for the present study was purchased from Millipore Corporation (USA). It is a 75% porous hydrophobic polyvinylidene fluoride (PVDF) membrane with a nominal pore size of 0.22 μ m and 47 mm in diameter. The PVDF membrane thickness was determined using a digital micrometer (Mitutoyo 369–250, \pm 0.001 mm accuracy), being the average value 125 μ m. These membranes are characterized by their high chemical resistance, being previously used in other works as a supporting material for SILMs [10,26]. It is worth mentioning that the PVDF membranes used as supporting material have a maximum operating temperature of 358 K (manufacturer's data) so they are the limiting factor for the SILM high temperature performance. The gases used in the experiments were carbon dioxide (99.7 \pm 0.01 vol%) and nitrogen (99.999 \pm 0.001 vol%) provided by Air Liquide (Spain).

2.2. SILM preparation

The immobilization procedure has been previously described [27,28]. To immobilize the RTILs, the microporous PVDF membrane was introduced into a vacuum chamber for 1h in order to

remove the air from the pores and, therefore allowing an easier introduction of RTIL into their porous structure. Once the membrane was under vacuum for 1 h, drops of RTILs are spread out at the membrane surface using a syringe, while keeping the vacuum inside the chamber. Then the liquid excess on the membrane surface was wiped up softly with a tissue. The amount of liquid immobilized in the membrane was determined gravimetrically, and the increase of thickness was measured before and after the immobilization procedure.

2.3. Methods

The experimental setup used for the gas permeation experiments has been previously described elsewhere [27,28]. Basically, the SILM is placed over a stainless steel permeation cell leading to an effective membrane area about 14.05 cm². A driving force of around 0.45 bar was established and the pressure change was measured using two pressure transducers (Omega, UK). The temperature was maintained using a water bath.

Gas permeability through the SILM was determined according to Eq. (1):

$$\frac{1}{\beta} \ln \left(\frac{[P_{\text{feed}} - P_{\text{perm}}]_0}{[P_{\text{feed}} - P_{\text{perm}}]} \right) = \frac{1}{\beta} \ln \left(\frac{\Delta p_0}{\Delta p} \right) = P_{\text{SILM}} \frac{t}{\delta} \quad (1)$$

where p_{feed} and p_{perm} are the pressures in the feed and permeate compartments, respectively; β a geometric parameter (1188.9 m⁻¹); P_{SILM} the permeability through the membrane calculated under constant partial pressure difference; t the time and δ is the membrane thickness. The ideal selectivity can be calculated by the ratio between the permeabilities of two pure different gases.

CO₂ solubility was evaluated using a TGA-60H Shimadzu Thermobalance where simultaneous thermogravimetric/differential (TG/DTA) analyses were performed. A molecular sieve trap was installed to remove traces of water from the feed gas. The sample temperature was measured with an accuracy of ± 0.1 K and the TG sensitivity was about 1 μg . The experimental conditions were a CO₂ flow rate of 50 mL min⁻¹, temperatures from 298 to 333 K and atmospheric pressure.

Once determined the gas permeability through the membrane and CO₂ solubility in the RTIL, the effective diffusion coefficients can be calculated considering that gas transport occurs via solution–diffusion mechanism according to Eq. (2):

$$P_{\text{SILM}} = S D_{\text{eff}} \quad (2)$$

where P_{SILM} is the permeability through the membrane; S is the gas solubility and D_{eff} the effective diffusion coefficient.

3. Results and discussion

3.1. Permeability

The experimental permeability results obtained in the present work are based on the following assumption: gas transport takes place entirely in the RTIL since the polyvinylidene fluoride (PVDF) support has very low permeabilities of 2.7 and 0.4 barrers for CO₂ and N₂ respectively. The SILMs permeabilities are between 325 barrers (CO₂) and 61.5 barrers (N₂) times greater in magnitude. Therefore, the assumption that the RTIL is the main contributor to gas permeability when comparing with the support is valid. The temperature effect on CO₂ and N₂ permeability as well as the CO₂/N₂ ideal selectivity was studied in the range of temperatures from 298 to 333 K. Table 2 shows the experimental CO₂ and N₂ permeability through the acetate based SILMs. The CO₂ permeance values for these membranes are in the order of 852–2114 barrers and CO₂/N₂ selectivity ranges between 26

Table 2
Experimental CO₂ and N₂ permeability through SILMs.

RTIL	T (K)	298	303	313	323	333
[Emim][Ac]	P_{CO_2} (barrer)	878.8	1118.1	1329.0	1721.3	2064.9
	P_{N_2} (barrer)	26.1	32.5	41.3	58.3	78.1
	$P_{\text{CO}_2}/P_{\text{N}_2}$	33.7	34.4	32.2	29.5	26.4
[Bmim][Ac]	P_{CO_2} (barrer)	851.9	1005.3	1269.2	1601.5	1940.9
	P_{N_2} (barrer)	24.6	29.5	37.8	50.7	65.3
	$P_{\text{CO}_2}/P_{\text{N}_2}$	34.6	34.1	33.6	31.6	29.7
[Vbtma][Ac]	P_{CO_2} (barrer)	1100	1305.6	1536.2	1828.3	2114.2
	P_{N_2} (barrer)	28.2	36.1	48.3	61.8	77.5
	$P_{\text{CO}_2}/P_{\text{N}_2}$	39.0	36.2	31.8	29.6	27.3

and 39. According to the experimental research, the effect of the cation on gas permeability is negligible when comparing with the anion. The SILMs studied in this work displays higher permeability values when comparing to polymeric membranes reported in literature generally below 1000 barrers [6–11]. Moreover, the results are in good agreement with those reported by Shi et al. [21] for the separation CO₂/H₂ in [Emim][Ac] based SILMs showing CO₂ permeabilities from 1325 to 3701 barrers in the temperature range 310–373 K.

An increase in gas permeability is observed as a result of the temperature increase. The logarithm of the permeability follows a linear relationship with the inverse of the temperature as it is shown in Fig. 2; therefore, the temperature influence on the gas permeability is well described in terms of an Arrhenius type relationship by Eq. (3):

$$P = P_0 \exp(-E_p/RT) \quad (3)$$

where P_0 is the pre-exponential factor and E_p the activation energy of permeation.

The activation energies of permeation for CO₂ and N₂ are reported in Table 3. These results are in good agreement with the previous literature data [29–32].

The activation energies of CO₂ permeation is in the range of previous values reported in the literature using different commercial polymeric supports [21,29]. The differences in the CO₂ activation energies of permeation between the polymeric and the inorganic supports may be due to the greater porosity of the polymeric support (75–85%) compared to 25–50% for the alumina leading to a decrease in the membrane volume occupied by the RTILs. The activation energies of N₂ permeation are higher than those found for CO₂ as it is shown in Table 3, which justifies a negative influence of the temperature in the selectivity.

The CO₂/N₂ ideal selectivities in the SILMs are plotted in Fig. 3 as a function of the temperature. An increase in temperature leads to a decrease in the ideal CO₂/N₂ selectivity according with the activation energies.

Comparing the permeability results at increasing temperatures to the upper-bound values for the selectivity vs. permeability of polymer membranes for CO₂/N₂ separation given by Robeson [5] it can be concluded that most of these SILMs have better performance than many polymer membranes previously studied, being the experimental results near the upper bound as it is shown in Fig. 4.

3.2. Solubility

Table 4 shows the CO₂ solubility in molar fraction in the three studied ionic liquids. The solubility data are in good agreement

with values previously reported in the literature at the same experimental conditions for [Emim][Ac] and [Bmim][Ac] [14–16].

The solubility dependence with temperature is typically written in terms of the van't Hoff relationship according to Eq. (4):

$$S = S_0 \exp(-\Delta H_s/RT) \quad (4)$$

where S_0 is the pre-exponential factor and ΔH_s is the partial molar enthalpy of absorption. The natural logarithm of the solubility follows a linear relationship with the inverse of temperature as shown in Fig. 5. The CO₂ partial molar enthalpy of absorption, ΔH_s , is reported in Table 5. The negative values of the absorption enthalpy corresponds to the exothermic behavior of the process. These values are in good agreement with the literature [29,32,33]. Taking into account the positive influence of the temperature in the diffusivity an endothermic absorption could be better in order to increase the permeability with the temperature.

3.3. Diffusivity

The calculation of CO₂ diffusivity from permeability and solubility, both measured and adjusted by linear fitting, it is possible considering that gas transport occurs via solution–diffusion mechanism where the permeability of a gas through the SILM (P_{SILM}) is the product of its solubility in the membrane (S) and effective diffusivity (D_{eff}) by applying Eq. (2) [34]. The permeability in cm² s⁻¹, P_{SILM} , and the dimensionless solubility, H , are calculated according to Appendix A. The estimated diffusion coefficients cm² s⁻¹ for CO₂ in the studied RTILs are presented in Table 6.

The Arrhenius equation describes well the relationship between gas diffusivity and temperature as it is shown in Fig. 6

$$D = D_0 \exp(-E_D/RT) \quad (5)$$

where D_0 is the pre-exponential factor and E_D the activation energy of diffusion. The activation energies of diffusion, E_D , are

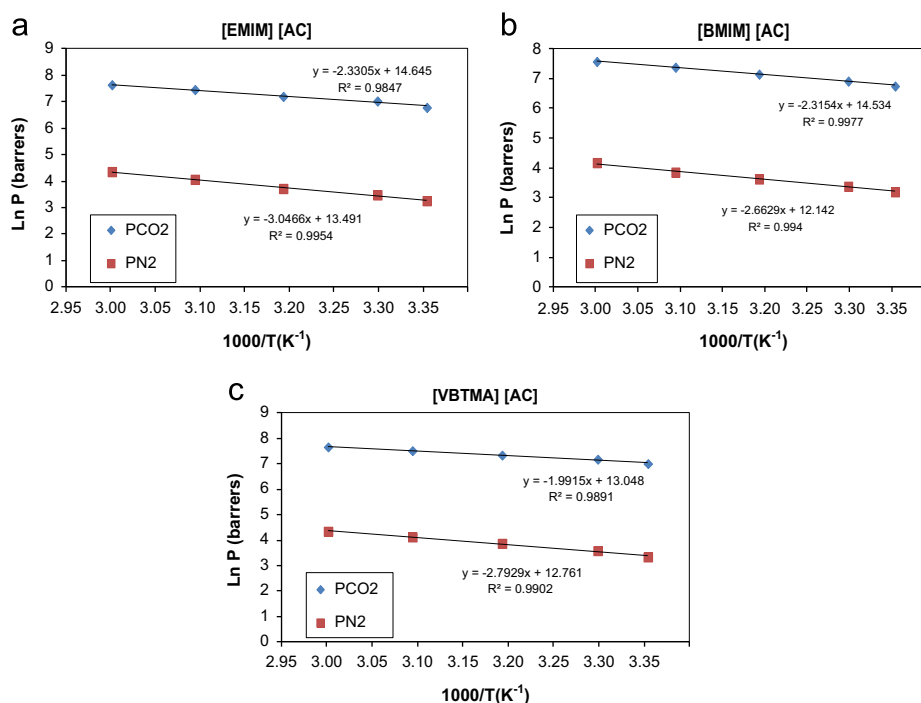


Fig. 2. Natural logarithm of CO₂ and N₂ permeability through [Emim][Ac] (a), [Bmim][Ac] (b) and [Vbtma][Ac] (c) plotted against the inverse of the temperature. Solid lines are the linear regression of the data.

Table 3

Experimental and literature activation energies of permeation, E_p .

Support	Gas	RTIL	E_p (kJ/mol)	Reference
Polyvinylidene fluoride (PVDF)	CO ₂	[Emim][Ac]	19.37	Present work
Polyvinylidene fluoride (PVDF)	N ₂	[Emim][Ac]	25.32	Present work
Polyvinylidene fluoride (PVDF)	CO ₂	[Bmim][Ac]	19.25	Present work
Polyvinylidene fluoride (PVDF)	N ₂	[Bmim][Ac]	22.13	Present work
Polyvinylidene fluoride (PVDF)	CO ₂	[Vbtma][Ac]	16.55	Present work
Polyvinylidene fluoride (PVDF)	N ₂	[Vbtma][Ac]	23.22	Present work
Polysulfone (PSF)	CO ₂	[Hmim][Te ₂ N]	17.38	Ilconich et al. [29]
Polysulfone (PSF)	He	[Hmim][Te ₂ N]	5.35	Ilconich et al. [29]
Alumina	CO ₂	[Hmim][Te ₂ N]	8.03	Adibi et al. [30]
Alumina	CH ₄	[Hmim][Te ₂ N]	29.35	Adibi et al. [30]
Polysulfone (PSF)	CO ₂	[Emim][Ac]	25.47	Shi et al. [21]
Polysulfone (PSF)	H ₂	[Emim][Ac]	16.02	Shi et al. [21]
α -Alumina	CO ₂	[Bmim][Bf ₄]	7.5	Iarikov et al. [31]
α -Alumina	CH ₄	[Bmim][Bf ₄]	20	Iarikov et al. [31]

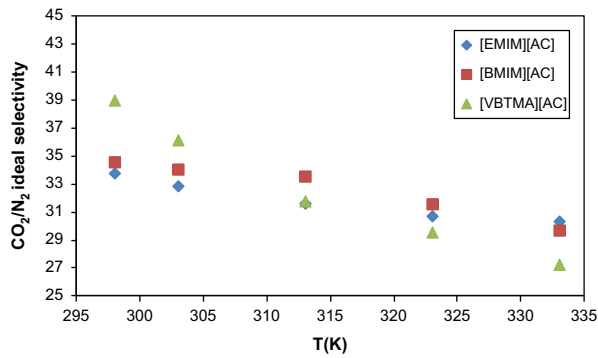


Fig. 3. Temperature influence on CO₂/N₂ selectivity.

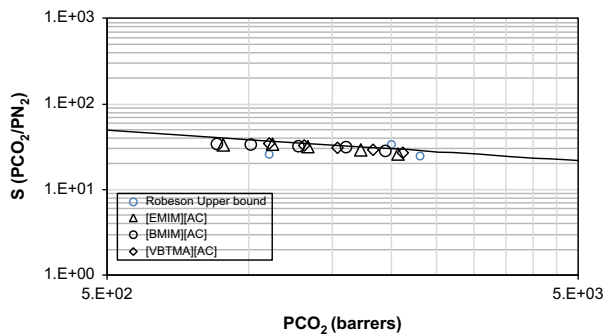


Fig. 4. Upper bound correlation for CO₂/N₂ separation.

Table 4
CO₂ solubility data in acetate based ionic liquids.

T (K)	RTIL		
	[EMIM][Ac]	[BMIM][Ac]	[VBTMA][Ac]
298.15	0.267	0.273	0.351
303.15	0.257	0.255	0.325
313.15	0.231	0.225	0.283
323.15	0.212	0.195	0.241
333.15	0.189	0.171	0.210

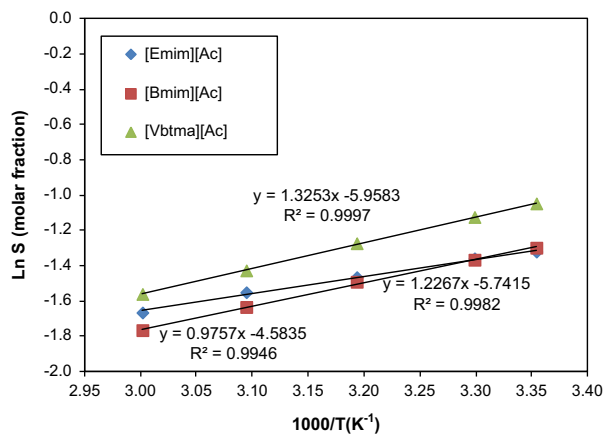


Fig. 5. Natural logarithm of CO₂ solubility plotted against the inverse of the temperature. Solid lines are the linear regression of the data.

reported in Table 7. These values are consistent with those values found in the literature [29,30,35–38].

According to our results, the activation energy for the permeability is the algebraic sum of the activation energy for the

Table 5
Experimental and literature ΔH_s data.

RTIL	ΔH _s (kJ/mol)	Reference
[Emim][Ac]	−8.29	Present work
[Bmim][Ac]	−10.19	Present work
[Vbtma][Ac]	−11.02	Present work
[Hmim][Tf ₂ N]	−11.19	Ikonich et al. [29]
[Bmim][Pf ₆]	−14.30	Anthony et al. [32]
[Bmim][Pf ₄]	−13.90	Anthony et al. [32]
[Bmim][Tf ₂ N]	−12.50	Anthony et al. [32]
[MeBuPyrr][Tf ₂ N]	−11.90	Anthony et al. [32]
[Bmim][Pf ₆]	−16.10	Cadena et al. [33]
[Bmmim][Pf ₆]	−13.00	Cadena et al. [33]
[Bmim][Pf ₄]	−15.90	Cadena et al. [33]
[Bmmim][Bf ₄]	−14.50	Cadena et al. [33]
[Emim][Tf ₂ N]	−14.20	Cadena et al. [33]
[Emmim][Tf ₂ N]	−14.70	Cadena et al. [33]

Table 6
Diffusivity calculated data.

RTIL	T (K)	298	303	313	323	333
[Emim][Ac]	10 ⁵ P (cm ² /s)	0.73	0.94	1.16	1.55	1.91
	H (−)	0.0237	0.0244	0.0263	0.02880	0.0306
	10 ⁷ D (cm ² /s)	1.73	2.30	3.05	4.33	5.86
[Bmim][Ac]	10 ⁵ P (cm ² /s)	0.71	0.85	1.11	1.44	1.80
	H (−)	0.0282	0.0299	0.0329	0.0370	0.0412
	10 ⁷ D (cm ² /s)	1.99	2.53	3.64	5.33	7.41
[Vbtma][Ac]	10 ⁵ P (cm ² /s)	0.91	1.10	1.34	1.64	1.96
	H (−)	0.027	0.0287	0.0319	0.0365	0.0407
	10 ⁷ D (cm ² /s)	2.46	3.17	4.28	6.01	7.99

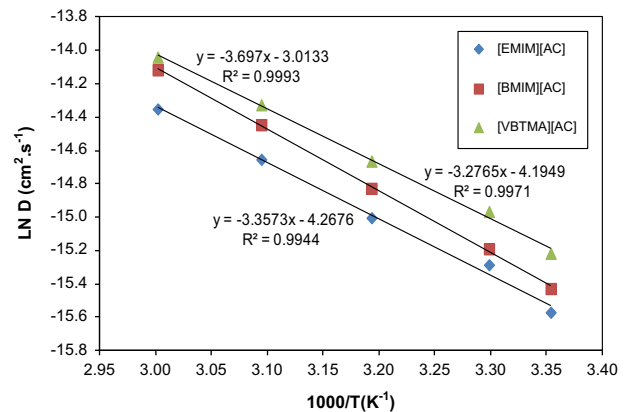


Fig. 6. Natural logarithm of CO₂ diffusivity vs. the inverse of the temperature for the studied RTILs. Solid lines are the linear regression of the data.

diffusivity and the partial molar enthalpy of absorption therefore, the influence of the temperature in the permeability is described by an exponential Arrhenius type equation, with an activation energy including the influence of the temperature in the effective diffusivity and in the solubility.

4. Conclusions

In this work, CO₂ and N₂ permeabilities through SILMs were determined at temperatures ranging from 298 to 333 K. Gas permeability increases with the temperature while CO₂/N₂ selectivity decreases with an increase in temperature for all the studied

Table 7
Calculated and literature E_D data.

Gas	RTIL	E_D (kJ/mol)	Reference
CO ₂	[Emim][Ac]	27.91	Present work
CO ₂	[Bmim][Ac]	30.74	Present work
CO ₂	[Vbtma][Ac]	27.24	Present work
CO ₂	[Hmim][Tf ₂ N]	16.42	Ilconich et al. [29]
CO ₂	[Bmpy][Bf ₄]	21	Morganty and Baltus [35]
CO ₂	[Omim][Bf ₄]	18	Morganty and Baltus [35]
CO ₂	[Hmim][Bf ₄]	22	Morganty and Baltus [35]
CO ₂	[Hmim][Tf ₂ N]	14	Morganty and Baltus [35]
CO ₂	[Emim][Tf ₂ N]	8	Morganty and Baltus [35]
CO ₂	[Emim][Beti]	14	Morganty and Baltus [35]
CO ₂	[Emim][Tfa]	11	Morganty and Baltus [35]
CO ₂	[Emim][TfO]	14	Morganty and Baltus [35]
CO ₂	[Bmim][Tf ₂ N]	10	Morganty and Baltus [35]
CO ₂	[Pmmim][Tf ₂ N]	15	Morganty and Baltus [35]
CO ₂	[Bmpy][Tf ₂ N]	12	Morganty and Baltus [35]
CO ₂	[Bmim][Bf ₄]	6	Morganty and Baltus [35]
CO ₂	[Bmim][Pf ₆]	27.2	Shiflett and Yokozeki [36]
CO ₂	[Bmim][Bf ₄]	24.3	Shiflett and Yokozeki [36]
CO ₂	[Bmim][Pf ₆]	47.72	Barghi et al. [37]
CH ₄	[Bmim][Pf ₆]	61.11	Barghi et al. [37]
CO ₂	[Hmim][Tf ₂ N]	21.50	Adibi et al. [30]
CH ₄	[hmim][Tf ₂ N]	33.29	Adibi et al. [30]
CO ₂	[Emim][Tf ₂ N]	16.9	Morgan et al. [38]
CO ₂	[Bmim][Beti]	22.3	Morgan et al. [38]

RTILs. The permeability activation energies are higher for nitrogen than for carbon dioxide.

Acetate based SILMs are useful for CO₂/N₂ separation since the results obtained in this work are near the Robeson upper bound corresponding to the best polymeric materials.

Gas diffusion coefficients were estimated assuming that gas permeation occurs via a solution–diffusion mechanism ($P=DS$) and the activation energies for the permeability, solubility and diffusivity were calculated. The experimental results of the activation energies and the absorption enthalpies agree well with the previous literature results.

In order to get a higher influence of the temperature in the permeability, it is recommended the introduction of RTILs with an endothermic absorption, which may increase the permeability activation energy.

Acknowledgments

The authors gratefully acknowledge the financial support from the Spanish Ministry of Economy and Competitiveness Project ENE 2010-14828 and Project CTQ2008-00690.

Appendix A. Diffusivity

Permeability data is often expressed in barrer according to

$$1 \text{ barrer} = \frac{10^{-10} \text{ cm}^3 \text{ gas (STP) (cm_thickness)}}{(\text{cm}^2 \text{_membrane area}) (\text{cmHg_pressure}) \text{ s}} \quad (\text{A.1})$$

(STP=273.15 K and 1.01325×10^5 Pa)

The equivalence in $\text{cm}^2 \text{ s}^{-1}$ is defined as

$$1 \text{ barrer} = \frac{10^{-10} \text{ cm}^3 \text{ (STP) cm}}{\text{cm}^2 \text{ cmHg s}} \left[\frac{\text{mol (STP)}}{22.4 \times 10^3 \text{ cm}^3} \right] \times \left[62.36367 \frac{\text{mmHg}}{\text{mol K}} \frac{10^3 \text{ cm}^3}{1 \text{ L}} \frac{1 \text{ cmHg}}{10 \text{ mmHg}} \right] 298.15 \text{ K} \\ = 8.296 \times 10^{-9} \frac{\text{cm}^2}{\text{s}} \quad (\text{A.2})$$

The Henry's law constant has been calculated by means of the following equation [39]:

$$H = \frac{C_g^*}{C_l^*} = \frac{y^* \rho_g}{x^* \rho_l} = \frac{y^*}{x^*} \frac{P_T}{RT} = \frac{1}{S} \quad (\text{A.3})$$

where y^* and x^* are the molar fractions in the gas and liquid phases respectively, being in equilibrium with themselves; ρ_l is the molar density of the liquid and P_T the total pressure.

Nomenclature

D_{eff}	effective diffusion coefficient ($\text{cm}^2 \text{ s}^{-1}$)
D_0	pre-exponential factor of diffusion ($\text{cm}^2 \text{ s}^{-1}$)
E_D	activation energy of diffusion (kJ mol^{-1})
E_p	activation energy of permeation (kJ mol^{-1})
H	Henry's law constant (–)
P_0	pre-exponential factor of gas permeability (barrer)
P_{SILM}	gas permeability through the membrane (barrer)
P_T	total pressure (bar)
p_{feed}	pressure in the feed compartment (Pa)
p_{perm}	pressure in the permeate compartment (Pa)
R	ideal gas constant ($\text{bar L mol}^{-1} \text{ K}^{-1}$)
S	gas solubility (molar fraction)
S_0	pre-exponential factor of gas solubility (molar fraction)
T	temperature (K)
t	time (s)
x^*	liquid molar fraction
y^*	gas molar fraction in equilibrium with liquid

Greek letters

β	geometric factor (m^{-1})
δ	membrane thickness (m)
ρ_l	molar density of the liquid (mol L^{-1})
ΔH_s	partial molar enthalpy of absorption (kJ mol^{-1})

References

- [1] K.R. Seddon, Ionic liquids for clean technology, *J. Chem. Technol. Biotechnol.* 68 (1997) 351–356.
- [2] F.J. Hernández-Fernández, A.P. de los Ríos, F. Tomás-Alonso, J.M. Palacios, G. Villora, Preparation of supported ionic liquid membranes: influence of the ionic liquid immobilization method on their operational stability, *J. Membr. Sci.* 341 (2009) 172–177.
- [3] M.J. Earle, J.M.S.S. Esperança, M.A. Gilea, J.N. Canongia Lopes, L.P.N. Rebelo, J. W. Magee, K.R. Seddon, J.A. Widegren, The distillation and volatility of ionic liquids, *Nature* 439 (2006) 831–834.
- [4] P. Scovazzo, Determination of the upper limits, benchmarks, and critical properties for gas separations using stabilized room temperature ionic liquid membranes (SILMs) for the purpose of guiding future research, *J. Membr. Sci.* 343 (2009) 199–211.
- [5] L.M. Robeson, The upper bound revisited, *J. Membr. Sci.* 320 (2008) 390–400.
- [6] P. Scovazzo, J. Kieft, D.A. Finan, C. Koval, D. DuBois, R. Noble, Gas separations using non-hexafluorophosphate [PF₆][–] anion supported ionic liquid membranes, *J. Membr. Sci.* 238 (2004) 57–63.
- [7] J.E. Bara, T.K. Carlisle, C.J. Gabriel, D. Camper, A. Finotello, D.L. Gin, R.D. Noble, Guide to CO₂ separations in imidazolium-based room-temperature ionic liquids, *Ind. Eng. Chem. Res.* 48 (2009) 2739–2751.
- [8] P. Scovazzo, D. Havard, M. McShea, S. Mixon, D. Morgan, Long-term, continuous mixed-gas dry fed CO₂/CH₄ and CO₂/N₂ separation performance and selectivities for room temperature ionic liquid membranes, *J. Membr. Sci.* 327 (2009) 41–48.
- [9] P. Cserjési, N. Nemestóthy, K. Bélafi-Bakó, Gas separation properties of supported liquid membranes prepared with unconventional ionic liquids, *J. Membr. Sci.* 349 (2010) 6–11.
- [10] L.A. Neves, J.G. Crespo, I.M. Coelho, Gas permeation studies in supported ionic liquid membranes, *J. Membr. Sci.* 357 (2010) 160–170.

- [11] P. Jindaratamee, Y. Shimoyama, H. Morizaki, A. Ito, Effects of temperature and anion species on CO₂ permeability and CO₂/N₂ separation coefficient through ionic liquid membranes, *J. Chem. Thermodyn.* 43 (2011) 311–314.
- [12] E.J. Maginn, Design and evaluation of ionic liquids as novel CO₂ absorbents, (<http://www.netl.doe.gov/technologies/coalpower/ewr/CO2/pubs>), 2013 (accessed 24.01.13).
- [13] D. Chinn, D.Q. Vu, M.S. Driver, L.C. Boudreau, CO₂ removal from gas using ionic liquid absorbents, US Patent US20,060,251,558A1, 2006, November 9; US20,050,129,598A1, 2005, June 16.
- [14] M.B. Shiflett, D.J. Kasprzak, A. Yokozeki, Phase behavior of {carbon dioxide + [bmim][Ac]} mixtures, *J. Chem. Thermodyn.* 40 (2008) 25–31.
- [15] A. Yokozeki, M.B. Shiflett, L.M. Grieco, T. Foo, Physical and chemical absorptions of carbon dioxide in room-temperature ionic liquids, *J. Phys. Chem. B* 112 (2008) 16654–16663.
- [16] M.B. Shiflett, A. Yokozeki, Phase behavior of carbon dioxide in ionic liquids: [emim][Acetate], [emim][Trifluoroacetate], and [emim][Acetate] + [emim][Trifluoroacetate] mixtures, *J. Chem. Eng. Data* 54 (2009) 108–114.
- [17] M.B. Shiflett, B.A. Elliott, A.M.S. Niehaus, A. Yokozeki, Separation of N₂O and CO₂ using room-temperature ionic liquid [bmim][Ac], *Sep. Sci. Technol.* 47 (2012) 411–421.
- [18] M.B. Shiflett, A.M.S. Niehaus, B.A. Elliott, A. Yokozeki, Phase behavior of N₂O and CO₂ in room-temperature ionic liquids [bmim][Tf₂N], [bmim][BF₄], [bmim][N(CN)₂], [bmim][Ac], [eam][NO₃], and [bmim][SCN], *Int. J. Thermophys.* 33 (2012) 412–436.
- [19] B.L. Bhargava, S. Balasubramanian, Probing anion–carbon dioxide interactions in room temperature ionic liquids: gas phase cluster calculations, *Chem. Phys. Lett.*, 444, 2007, 2007; 242–246.
- [20] J.A. Steckel, Ab initio calculations of the interaction between CO₂ and the acetate ion, *J. Phys. Chem. A* 116 (2012) 11643–11650.
- [21] W. Shi, C.R. Myers, D.R. Luebke, J.A. Steckel, D.C. Sorescu, Theoretical and experimental studies of CO₂ and H₂ separation using the 1-ethyl-3-methylimidazolium acetate ([emim][CH₃COO]) ionic liquid, *J. Phys. Chem. B* 116 (2012) 283–295.
- [22] S. Supasitmongkol, P. Styrring, High CO₂ solubility in ionic liquids and a tetraalkylammonium-based poly(ionic liquid), *Energy Environ. Sci.* 3 (2010) 1961–1972.
- [23] R.S. Bhavsar, S.C. Kumbharkar, U.K. Kharul, Polymeric ionic liquids (PILs): effect of anion variation on their CO₂ sorption, *J. Membr. Sci.* 389 (2012) 305–315.
- [24] M.G. Freire, A.R.R. Teles, M.A.A. Rocha, B. Schroder, C.M.S.S. Neves, P. J. Carvalho, D.V. Evtuguin, L.M.N.B.F. Santos, J.A.P. Coutinho, Thermophysical characterization of ionic liquids able to dissolve biomass, *J. Chem. Eng. Data* 56 (2011) 4813–4822.
- [25] E.J. Maginn, Design and evaluation of ionic liquids as novel CO₂ absorbents, , 2005. (Quarterly Technical Report, January 2005 (DE-FG26-04NT42122)).
- [26] R. Fortunato, L.C. Branco, C.A.M. Afonso, J. Benavente, J.G. Crespo, Electrical impedance spectroscopy characterisation of supported ionic liquid membranes, *J. Membr. Sci.* 270 (2006) 42–49.
- [27] J. Albo, E. Santos, L.A. Neves, S.P. Simeonov, C.A.M. Afonso, J.G. Crespo, A. Irabien, Separation performance study of CO₂ through Supported Magnetic Ionic Liquid Membranes (SMILMs), *Sep. Purif. Technol.* 97 (2012) 26–33.
- [28] E. Santos, J. Albo, C.I. Daniel, C.A.M. Portugal, J.G. Crespo, A. Irabien, Permeability modulation of Supported Magnetic Ionic Liquid Membranes (SMILMs) by an external magnetic field, *J. Membr. Sci.* 430 (2013) 56–61.
- [29] J. Ilconich, C. Meyers, H. Pennline, D. Luebke, Experimental investigation of the permeability and selectivity of supported ionic liquid membranes for CO₂/He separation at temperatures up to 125 °C, *J. Membr. Sci.* 298 (2007) 41–47.
- [30] M. Adibi, S.H. Barghi, D. Rashtchian, Predictive models for permeability and diffusivity of CH₄ through imidazolium-based supported ionic liquid membranes, *J. Membr. Sci.* 371 (2011) 127–133.
- [31] D.D. Iarikov, P. Hacarlioglu, S.T. Oyama, Supported room temperature ionic liquid membranes for CO₂/CH₄ separation, *Chem. Eng. J.* 166 (2011) 401–406.
- [32] J.L. Anthony, J.L. Anderson, E.J. Maginn, J.F. Brennecke, Anion effects on gas solubility in ionic liquids, *J. Phys. Chem. B* 109 (2005) 6366–6374.
- [33] C. Cadena, J.L. Anthony, J.K. Shah, T.I. Morrow, J.F. Brennecke, E.J. Maginn, Why is CO₂ so soluble in imidazolium-based ionic liquids? *J. Am. Chem. Soc.* 126 (2004) 5300–5308.
- [34] R.C. Reid, J.M. Prausnitz, B.E. Poling, *The Properties of Gases and Liquids*, 4th ed., Mc Graw-Hill New York, 1987.
- [35] S.S. Morganty, R.E. Baltus, Diffusivity of carbon dioxide in room temperature ionic liquids, *Ind. Eng. Chem. Res.* 49 (2010) 9370–9376.
- [36] M.B. Shiflett, A. Yokozeki, Solubilities and diffusivities of carbon dioxide in ionic liquids: [bmim][PF₆] and [bmim][BF₄], *Ind. Eng. Chem. Res.* 44 (2005) 4453–4464.
- [37] S.H. Barghi, M. Adibi, D. Rashtchian, An experimental study on permeability, diffusivity, and selectivity of CO₂ and CH₄ through [bmim][PF₆] ionic liquid supported on an alumina membrane: investigation of temperature fluctuations effects, *J. Membr. Sci.* 362 (2010) 346–352.
- [38] D. Morgan, L. Ferguson, P. Scovazzo, Diffusivities of gases in room temperature ionic liquids: data and correlations obtained using a lag-time technique, *Ind. Eng. Chem. Res.* 44 (2005) 4815–4823.
- [39] R. Sander, Modeling atmospheric chemistry: interactions between gas-phase species and liquid cloud/aerosol particles, *Surv. Geophys.* 20 (1999) 1–31.